

On primordial universe in anti-de Sitter landscape

Pu-Xin Lin^{1,2*}, Hai-Long Huang^{1,3†}, Jun Zhang^{4‡}, and Yun-Song Piao^{1,3,4,5§}

¹ *School of Fundamental Physics and Mathematical Sciences,
Hangzhou Institute for Advanced Study, UCAS, Hangzhou 310024, China*

² *Department of Physics, University of Wisconsin-Madison,
1150 University Ave, Madison, WI 53706, U.S.A.*

³ *School of Physical Sciences, University of Chinese
Academy of Sciences, Beijing 100049, China*

⁴ *International Center for Theoretical Physics Asia-Pacific, Beijing/Hangzhou, China and*

⁵ *Institute of Theoretical Physics, Chinese Academy of Sciences,
P.O. Box 2735, Beijing 100190, China*

Abstract

How the spacetime evolved non-perturbatively in a landscape with multiple anti-de Sitter (AdS) vacua, which is theoretically well-motivated, has always been a matter of concern. As a step towards this issue, we perform (3+1)D numerical relativity simulations for the inhomogeneous universe in an AdS landscape, and find that large inhomogeneity of scalar field can develop into not only sphere-like bubbles, but also novel tube-like structures. It is observed that the bubble or tube wall (across the potential barrier) likely inflates as a quasi-dS space, while the different regions separated by the walls are in different AdS vacua and will collapse towards singularity.

PACS numbers:

* linpiaoxin17@mailsucas.ac.cn

† huanghailong18@mailsucas.ac.cn

‡ zhangjun@ucas.ac.cn

§ yspiao@ucas.ac.cn

I. INTRODUCTION

The success of inflation [1–5], consistent with current cosmological observations, suggests the existence of a de Sitter (dS) phase in the very early stage of our observable Universe. In string theory, although it is possible that dS vacua exist [6, 7], the construction of such vacua in string landscape is not straightforward. There are however valid concerns about the validity of such constructions in string theory, notably the swampland conjecture [8, 9], see also [10, 11] for recent reviews. In contrast, anti-de Sitter (AdS) vacua are easy to construct and are ubiquitous. Recently, it has been showed that AdS spacetime not only plays crucial roles as insights into our Universe, e.g.[12–17] but also have potential observable imprints [18–21].

The initial state of the universe might be highly inhomogeneous [22], i.e. the scalar field or spacetime metric can exhibit non-perturbative inhomogeneities before a region of space arrives at a certain vacuum, so that initially well-defined background in such highly inhomogeneous states does not exist. It is also often speculated that due to the past incompleteness of inflation [23], large fluctuations of spacetime will be inevitably excited near the initial cosmological singularity, in which case the initial conditions of scalar fields and spacetime are chaotic [5]. In such a non-perturbatively and highly inhomogeneous spacetime, perturbative calculation is not applicable any more.

In the past decades, numerical relativity (NR) has developed significantly and has been applied to studies on the merging of black hole binaries [24–26] and non-perturbative cosmologies, e.g.[27–31]. As pointed out, the study of AdS landscape is theoretically well-motivated. It is well-known that the region in a single AdS vacuum is unstable and will eventually collapse into a singularity [32], see also e.g.[33]. Consequently, the non-perturbative evolution of the entire spacetime in such landscape has continued to be a matter of concern, e.g.[34].

As a step towards this issue, we perform (3+1)D NR simulations of the “universe” in a simplified AdS landscape. Despite the application of NR simulations in cosmologies [27, 28, 35–37], few focused on the AdS landscape. Specially, in Ref. [37], we investigate the evolution of scalar field in an initial inhomogeneous expanding Universe and how a patch of spacetime evolves into the dS vacua that should happen at the early epoch of the Universe. In this letter, we further investigate the spacetime evolves in a landscape with multiple AdS

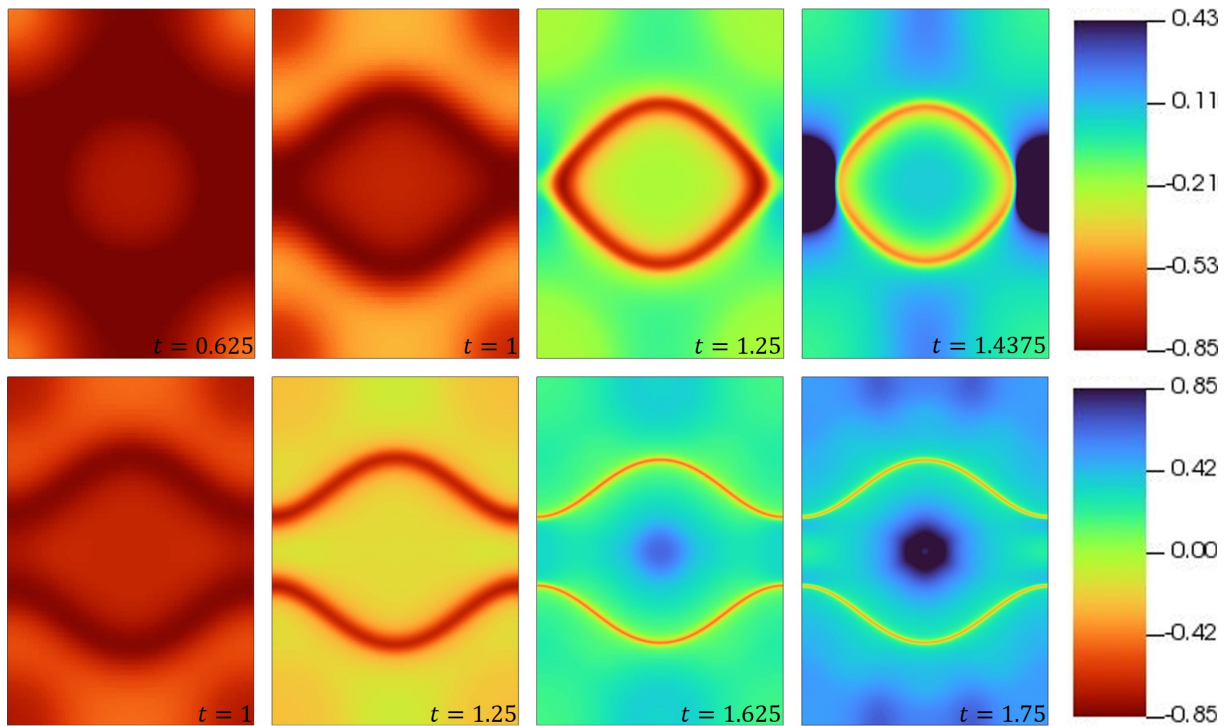


FIG. 1: **Snapshots of spacetime.** The upper and lower panel show how the sphere-like bubbles ($\phi_0 = 0.89$) and tube-like structures ($\phi_0 = 0.92$) form respectively, which are seen in light of the plane passing the center of the grid with normal $\vec{n} = (1, -1, 0)$. Initially, the whole space is expanding ($K < 0$ at the red end of the colorbar). After a period of evolution, different regions of space will be separated by expanding walls (the bubble wall or tube-like “ribbon” at which $K < 0$) into different AdS vacua, while the corresponding AdS regions will collapse ($K > 0$ with a blue shifted color).

vacua, which are more generic in string theory. We explore potential new phenomenology and investigate whether a quasi-de Sitter space can emerge on the bubble wall separating different AdS regions. Our simulation results show novel phenomena not captured by conventional perturbative analyses, see Fig.1, which in certain sense highlights the important role of NR in comprehending the non-perturbative phenomena of spacetime.

II. METHOD

Throughout this work, we consider a 1D potential as a phenomenological simplification of the actual complex AdS landscape, setting a fourth-order polynomial barrier between the

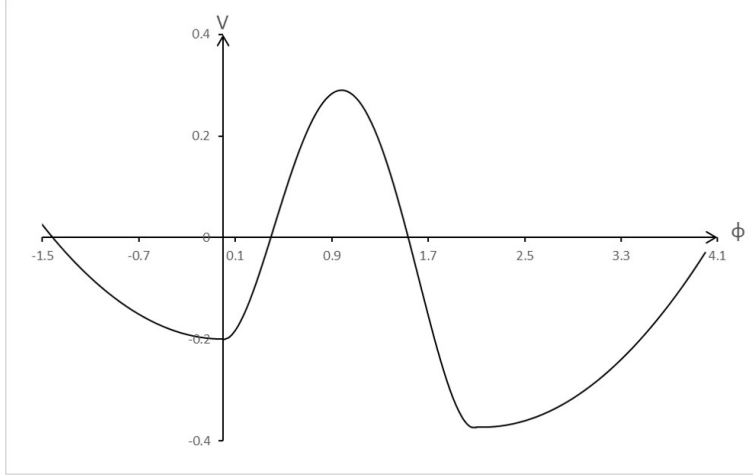


FIG. 2: **A simplified AdS landscape.** The effective potential $V(\phi)$ has two AdS minima separated by a potential barrier with positive energy.

two AdS minima that have quadratic forms $\sim \phi^2$ (see Fig.2),

$$V(\phi) = \begin{cases} \frac{1}{2}m_1^2(\phi - \phi_1)^2 + V_1, & \phi < \phi_1, \\ \lambda \left(\phi^2 + \frac{1}{\lambda}\right)^2 - 2\phi^3 - \frac{1}{\lambda} + V_1, & \phi_1 \leq \phi \leq \phi_2, \\ \frac{1}{2}m_2^2(\phi - \phi_2)^2 + V_2, & \phi_2 < \phi, \end{cases} \quad (1)$$

where $V_1, V_2 < 0$. Here, we set $m_1^2 = m_2^2 = 0.2$, $\lambda = 0.49$ ($c = \hbar = 8\pi G = 1$). We thus have the AdS-like vacua located at $\phi_1 = 0$ and $\phi_2 \simeq 2$, where the potential is constructed to be differentiable, and the maximal value of potential barrier is at $\phi_b \simeq 1$.

The large non-perturbative inhomogeneity of fields will be excited inevitably near the initial singularity or the Planck scale, giving rise to the possibility of initially configuration $\partial_i \phi \partial^i \phi \lesssim 1$, or $\Delta\phi \lesssim 1$. As example, we set the initial inhomogeneity of scalar field as

$$\phi|_{t=0} = \phi_0 + \Delta\phi \sum_{\vec{x}=x,y,z} \cos\left(\frac{2\pi\vec{x}}{L}\right), \quad (2)$$

where the amplitude of inhomogeneity is $\Delta\phi = \mathcal{O}(0.1)$, the wavelength of inhomogeneity is taken to be equal to the length of the periodic cubic region (in our simulation $L = 4$). In our simulation, we set the periodic boundary condition¹, and $\Delta\phi = 0.4$ is the default value unless otherwise specified, with ϕ_0 varying from 0.8 to 0.98.

¹ However, we also consider the reflective boundary condition with the GRChombo code, and still observed similar results. The details will be provided upon request.

We modify the BSSN based [38, 39] NR package GRChombo² [40] to perform the simulation. The NR simulation is usually performed in the 3+1 decomposition context for spacetime, with the metric as $g_{00} = -\alpha^2 + \beta_i\beta^i$, $g_{0i} = \beta_i$ and $g_{ij} = \gamma_{ij}$, where α is the lapse parameter, β^i the shift vector and γ_{ij} the spatial metric, while for the numerical stability, the spatial metric γ_{ij} must be further factorized into its determinant χ (conformal factor) and a comformal metric $\tilde{\gamma}_{ij} = \chi\gamma_{ij}$. The evolutions of $\tilde{\gamma}_{ij}$, the connections $\tilde{\Gamma}^i = \tilde{\gamma}^{jk}\tilde{\Gamma}_{jk}^i$ and the extrinsic curvature $K_{ij} = \frac{1}{3}K\delta_{ij} + A_{ij}$ comply with the BSSN equations [38, 39].

Initially, the values of the BSSN variables are set as $\tilde{\gamma}_{ij} = \delta_{ij}$, $\tilde{A}_{ij} = \chi A_{ij} = 0$, and $\chi = 1$. In GRChombo code [40], to satisfy the Hamiltonian constraint involving the scalar field, we enforce the constraint by relaxing the conformal factor in the light of $\partial_t\chi = \mathcal{H}$ ³, e.g. see recent Refs.[36, 37]. In addition, we set the initial scalar field at rest $\dot{\phi} = 0$, satisfying the momentum constraint and the initial expansion rate to be uniform $K_{init} = -\sqrt{3\langle\rho\rangle} \approx -1.08$, where $\langle\rho\rangle$ indicates the average initial energy density. In the special case of an isoptopic and homogeneous Universe, extrinsic curvature K is related to the Hubble constant as $K = -3H$ with geodesic observers.

III. RESULTS

The simulation results are presented in Fig.1 and Fig.3. The large inhomogeneity will spawn AdS bubbles in a background of a different AdS vacuum. As expected, if a bubble has subcritical initial radius, it will rapidly shrink and collapse into a black hole⁴, and eventually the whole space will evolve into a single AdS state and collapse integrally, see Fig.3-A. However, if the initial radii of the bubbles are supercritical, the regions with different AdS vacua will coexist, separated by not only near-spherical bubble walls (Fig.3-B) but also,

² <http://www.grchombo.org>

<https://github.com/GRChombo>

³ This parabolic equation evolves χ into a steady state $\partial_t\chi = \mathcal{H}$. It enforces the Hamiltonian constraint and thus prepares a proper initial condition. Here, the Hamiltonian constraint violation \mathcal{H} is given by

$$\mathcal{H} = \tilde{D}^2\chi - \frac{5}{4\chi}\tilde{\gamma}^{ij}\tilde{D}_i\chi\tilde{D}_j\chi + \frac{\chi}{2}\tilde{R} + \frac{1}{3}K^2 - \frac{\chi^3}{2}\tilde{A}^{ij}\tilde{A}_{ij} - \rho. \quad (3)$$

⁴ Using the Apparent Horizon Finder in GRChombo code, we find that the mass of the black hole is $M \approx 5.7$, which is associated with the apparent horizon and less than but converges to the actual mass of black hole.

interestingly, infinitely extending tube-like walls (Fig.3-C). Here, the critical radius of bubble refers to the minimal radius of bubble when the bubble phase can exist.

These tube-like walls can be understood more clearly in Fig.1. In our simulation, we replace an infinite space with the periodic boundary condition. This choice of boundary condition is motivated as follows: inhomogeneities occur at various scales, when considering evolution of those at a specific length scale, it is natural to expect the extent of the modes goes beyond just a single period. In light of this argument, the “bubble” in the lower panel of Fig.1 actually correspond to the tube that extend along $\vec{x}(=x, y, z)$ directions through the region where the periodicity of the initial perturbation modes persists. Such tube-like structure looks “as if” the adjacent spherical cells merged partly. It is intriguing to consider the more generic setup with perturbations at numerous wavelengths, a task beyond the scope of this letter, and to be pursued in future work.

It is significant to check the effect of the wavelength L of inhomogeneity (equivalently L/H_{init}^{-1}). A phase diagram is presented in Fig.4⁵. According to Fig.4, for $\phi_0/\phi_b \lesssim 0.9$, if $L/H_{init}^{-1} \lesssim 1$ (i.e. the wavelength L is “subhorizontal”), eventually the whole space will collapse integrally, while the bubble or tube phase comes into being only when the initial inhomogeneity is “superhorizontal” (the radius of the bubble is supercritical and superhorizontal). It is also worth noting that if $\phi_0/\phi_b \gtrsim 0.9$, i.e. ϕ_0 is close to the maximal value of potential barrier, we will see the bubble or tube phase for $L/H_{init}^{-1} \lesssim 1$ (the radius of the bubble is supercritical but subhorizontal).

Physically, our results can be qualitatively understood as follows. Here, if a bubble has subcritical initial radius, it will rapidly shrink and disappear, and eventually the whole space will evolve into a single AdS state and collapse integrally, while if a bubble has supercritical and superhorizontal initial radius, the collapse of bubble wall will be prevented by the expansion of wall spacetime, as expected theoretically in Ref.[34], so a bubble phase will come into being. As the initial radii of bubbles gets bigger (than a certain critical value), the bubbles will get closer so that they can partly join together through the tube naturally.

Here, the initial “universe” is set to be expanding homogeneously (all $H_{local} = const. > 0$), but eventually different regions will tend to evolve into different AdS vacua and be separated

⁵ Here, we fix the amplitude $\Delta\phi = 0.4$ of initial inhomogeneity. However, we actually also consider different $\Delta\phi = 0.3, 0.5$, but we find that the corresponding phase diagrams are essentially similar to Fig.4, only the slope of boundary lines separating the “Bubble” and “Tube” phases are different.

by bubble or tube walls. According to Fig.5, we see that though the AdS regions at both sides of the wall are collapsing, the existing walls will still expand and eventually arrive at a quasi-dS static profile, implying that the inflationary stage responsible for our observable Universe might happen at such walls, e.g.[41, 42].

It can be confirmed that in such AdS landscapes, inflation might occur. According to Refs.[41, 42], the width of the wall is $\delta_0 \sim (\phi_2 - \phi_1)V_b^{-1/2}$, and

$$\delta_0 > \frac{1}{H_0} \simeq \left(\frac{3}{V_b}\right)^{1/2} \quad (4)$$

must be satisfied for the inflation occurring on the wall. Here, considering the longitudinal Hubble parameter $H_L = -u^i u^j K_{ij}$ (u^i is the normal vector at the bubble wall), and $ds^2 = \gamma_{ij} e^i e^j dr^2 = \gamma^2 dr^2$ (r is the coordinate crossing the bubble wall and e^i is the direction vector at the wall), we have

$$\delta_0 \simeq \gamma \Delta r \gtrsim \frac{1}{H_L}, \quad (5)$$

see Fig.6, which confirms the condition (4).

IV. CONCLUSIONS

We performed full relativistic simulations for non-perturbative evolution of spacetime in a simple AdS landscape, and found that large inhomogeneity of a scalar field inclines to develop into sphere-like bubbles, and more unexpectedly, into tube-like structures. It is observed that the spacetime evolution is completely different in the AdS landscape, the bubble or tube walls might inflate forever as a quasi-dS space, while the different regions separated by the walls are in different AdS vacua and will collapse towards singularity.

Though we take a simple potential with two AdS minima as example, actually for a spacetime in a landscape with multiple AdS vacua, its local region always can be described as that with only two neighbouring AdS minima. Thus our results might have effectively captured some of the essentials of non-perturbative phenomenology of spacetime in AdS landscape. In this sense, further research on the NR simulations in a more realistic landscape for the early universe is interesting and required, which will help to deepen insight into the origin of our observable Universe.

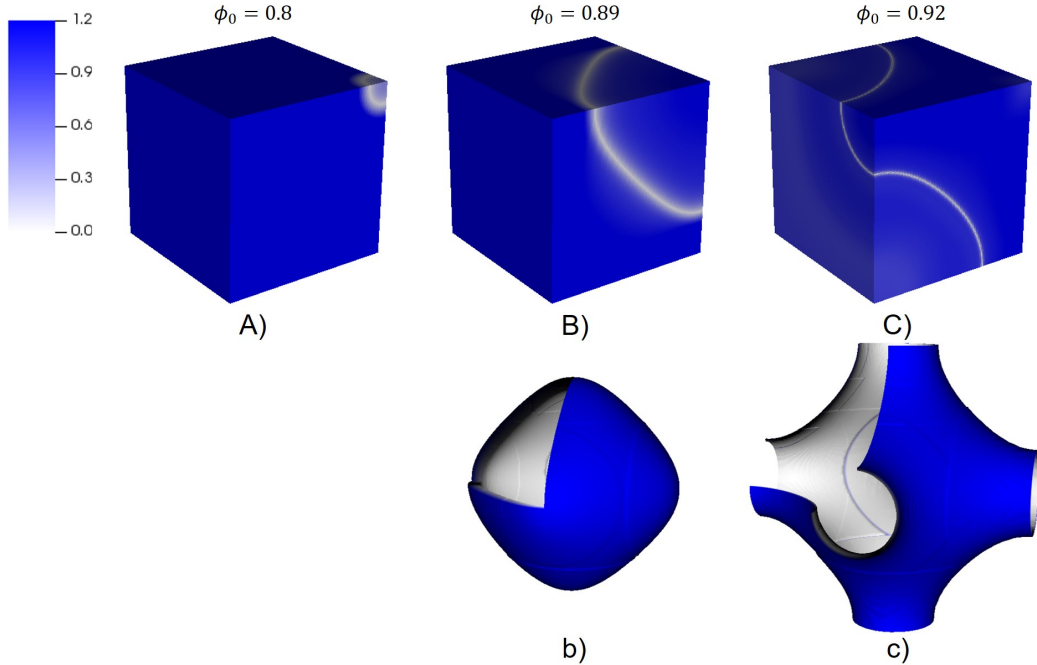


FIG. 3: **The value of $|\phi - \phi_b|$ (1/8 of the whole computational grid).** In subfig-A, B and C, the lower left and upper right regions correspond to the left and right side of the potential barrier in Fig.2, respectively, and the boundaries colored white mark the position of the barrier. In subfig-A, the snapshot is taken shortly before the upper right AdS region disappears. In subfig-B or C, the snapshot is taken when the bubble or tube wall eventually arrives at rest. The subfig-b and c show the interior of walls with 1/8 of the computational grid removed.

Acknowledgment This work is supported by the NSFC No.12075246 and by the Fundamental Research Funds for the Central Universities. We acknowledge the use of GRChombo code for our simulation and the Tianhe-2 supercomputer for providing computing resources. We would like to thank Tiago França, Hao-Hao Li and Hao-Yang Liu for useful discussions.

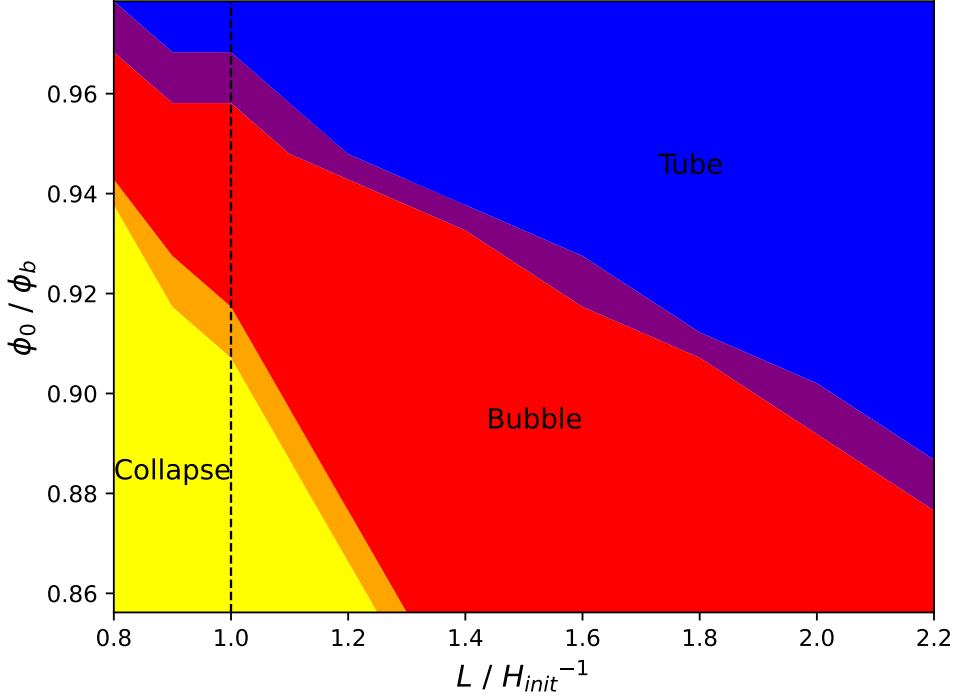


FIG. 4: **The phase diagram of bubble-tube Phase Transition.** “Collapse” represents the phase in which the whole space will collapse integrally, “Bubble” and “Tube” represent phases with existence of bubbles and tube-like structures respectively. The boundaries between them (indicated by the orange and purple strips) are not sharp since we cannot know which will be the final state in our simulation precision. Here, we mainly focus on the parameter space in which the wavelengths of initial inhomogeneity are very close to the initial horizon, $L \approx H_{init}^{-1}$, in order to see the Phase Transition between different phases.

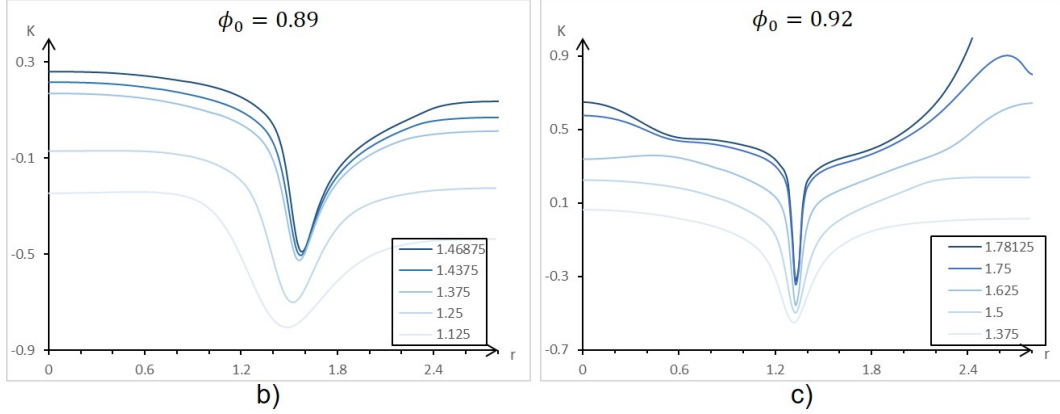


FIG. 5: **The evolution of extrinsic curvature scalar K .** The horizontal axis is the line from cubic center to the middle point on the edge of whole computational grids (upper right and left vertexes of the boxes in Fig.3). In subfig-b and c, the bubble and tube walls form, and eventually the walls will arrive a quasi-dS stationary profile ($K = const. < 0$ on wall).

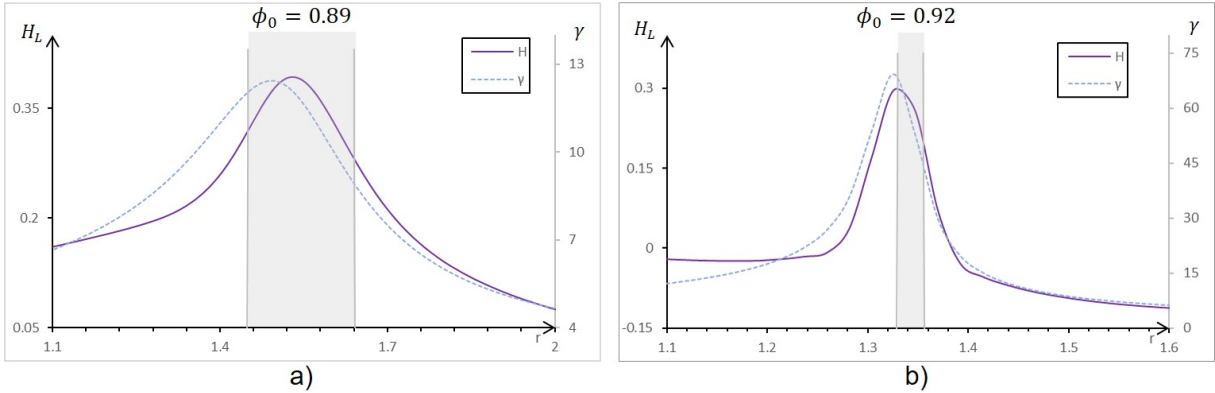


FIG. 6: **The longitudinal Hubble rate H_L and γ with respect to r across the bubble wall** for different initial conditions. The solid line is the longitudinal Hubble rate (value shown on the left vertical axis) and the dotted line is γ (value shown on the right axis).

-
- [1] A. H. Guth, Phys. Rev. D **23**, 347 (1981).
 - [2] A. D. Linde, Phys. Lett. B **108**, 389 (1982).
 - [3] A. Albrecht and P. J. Steinhardt, Phys. Rev. Lett. **48**, 1220 (1982).
 - [4] A. A. Starobinsky, Phys. Lett. B **91**, 99 (1980).
 - [5] A. D. Linde, Phys. Lett. B **129**, 177 (1983).

- [6] S. Kachru, R. Kallosh, A. D. Linde, and S. P. Trivedi, *Phys. Rev. D* **68**, 046005 (2003), hep-th/0301240.
- [7] R. Kallosh, A. Linde, E. McDonough, and M. Scalisi, *JHEP* **03**, 134 (2019), 1901.02022.
- [8] H. Ooguri and C. Vafa, *Nucl. Phys. B* **766**, 21 (2007), hep-th/0605264.
- [9] G. Obied, H. Ooguri, L. Spodyneiko, and C. Vafa (2018), 1806.08362.
- [10] T. D. Brennan, F. Carta, and C. Vafa, *PoS TASI2017*, 015 (2017), 1711.00864.
- [11] E. Palti, *Contemp. Phys.* **62**, 165 (2022).
- [12] Y. Chen, V. Gorbenko, and J. Maldacena, *JHEP* **02**, 009 (2021), 2007.16091.
- [13] T. Hartman, Y. Jiang, and E. Shaghoulian, *JHEP* **11**, 111 (2020), 2008.01022.
- [14] A. Levine and E. Shaghoulian (2022), 2204.08503.
- [15] S. Cooper, M. Rozali, B. Swingle, M. Van Raamsdonk, C. Waddell, and D. Wakeham, *JHEP* **07**, 065 (2019), 1810.10601.
- [16] S. Antonini, P. Simidzija, B. Swingle, and M. Van Raamsdonk (2022), 2203.11220.
- [17] S. Antonini, P. Simidzija, B. Swingle, and M. Van Raamsdonk (2022), 2206.14821.
- [18] G. Ye and Y.-S. Piao, *Phys. Rev. D* **101**, 083507 (2020), 2001.02451.
- [19] G. Ye and Y.-S. Piao, *Phys. Rev. D* **102**, 083523 (2020), 2008.10832.
- [20] J.-Q. Jiang and Y.-S. Piao, *Phys. Rev. D* **104**, 103524 (2021), 2107.07128.
- [21] G. Ye, J. Zhang, and Y.-S. Piao (2021), 2107.13391.
- [22] J. Feldbrugge, J.-L. Lehners, and N. Turok, *Phys. Rev. Lett.* **119**, 171301 (2017), 1705.00192.
- [23] A. Borde, A. H. Guth, and A. Vilenkin, *Phys. Rev. Lett.* **90**, 151301 (2003), gr-qc/0110012.
- [24] F. Pretorius, *Phys. Rev. Lett.* **95**, 121101 (2005), gr-qc/0507014.
- [25] M. Campanelli, C. O. Lousto, P. Marronetti, and Y. Zlochower, *Phys. Rev. Lett.* **96**, 111101 (2006), gr-qc/0511048.
- [26] J. G. Baker, J. Centrella, D.-I. Choi, M. Koppitz, and J. van Meter, *Phys. Rev. Lett.* **96**, 111102 (2006), gr-qc/0511103.
- [27] J. T. Giblin, J. B. Mertens, and G. D. Starkman, *Phys. Rev. Lett.* **116**, 251301 (2016), 1511.01105.
- [28] E. Bentivegna and M. Bruni, *Phys. Rev. Lett.* **116**, 251302 (2016), 1511.05124.
- [29] N. Musoke, S. Hotchkiss, and R. Easther, *Phys. Rev. Lett.* **124**, 061301 (2020), 1909.11678.
- [30] H. J. Macpherson, P. D. Lasky, and D. J. Price, *Phys. Rev. D* **95**, 064028 (2017), 1611.05447.
- [31] H. J. Macpherson, D. J. Price, and P. D. Lasky, *Phys. Rev. D* **99**, 063522 (2019), 1807.01711.

- [32] L. F. Abbott and S. R. Coleman, Nucl. Phys. B **259**, 170 (1985).
- [33] P. Bizon and A. Rostworowski, Phys. Rev. Lett. **107**, 031102 (2011), 1104.3702.
- [34] J. J. Blanco-Pillado, H. Deng, and A. Vilenkin, JCAP **05**, 014 (2020), 1909.00068.
- [35] W. E. East, M. Kleban, A. Linde, and L. Senatore, JCAP **09**, 010 (2016), 1511.05143.
- [36] K. Clough, E. A. Lim, B. S. DiNunno, W. Fischler, R. Flauger, and S. Paban, JCAP **09**, 025 (2017), 1608.04408.
- [37] P.-X. Lin and Y.-S. Piao, Phys. Rev. D **105**, 063534 (2022), 2111.09174.
- [38] T. W. Baumgarte and S. L. Shapiro, Phys. Rev. D **59**, 024007 (1998), gr-qc/9810065.
- [39] M. Shibata and T. Nakamura, Phys. Rev. D **52**, 5428 (1995).
- [40] K. Clough, P. Figueras, H. Finkel, M. Kunesch, E. A. Lim, and S. Tunyasuvunakool, Class. Quant. Grav. **32**, 245011 (2015), 1503.03436.
- [41] A. Vilenkin, Phys. Rev. Lett. **72**, 3137 (1994), hep-th/9402085.
- [42] A. D. Linde, Phys. Lett. B **327**, 208 (1994), astro-ph/9402031.